Journal of Neonatal Surgery
ISSN(Online): 2226-0439
Vol. 14, Issue 4s (2025)
https://www.jneonatalsurg.com

OPEN ACCESS

Clustering-Based Analysis of Meibomian Gland Morphology for Automated Assessment of Meibomian Gland Dysfunction Using the MGD-1k Dataset

Anantha Krishnan[*1], Md Salman Sarkar[2], Laxman Badavath[3]

[*1]School of Psychology and Sport Science, Adeilad Brigantia, Penrallt Rd, Bangor LL57 2AS, UK

[2]Faculty of Allied Health Sciences, SGT University, Gurgaon, India

[3]Ophthalmology Department, AIIMS MG Campus, Mangalagiri, Guntur District Andhra Pradesh – 522503

***Corresponding Author:**

(PhD),

Email ID: krishnananantha26@gmail.com

Cite this paper as: Anantha Krishnan, Md Salman Sarkar, Laxman Badavath, (2025) Clustering-Based Analysis of Meibomian Gland Morphology for Automated Assessment of Meibomian Gland Dysfunction Using the MGD-1k Dataset. *Journal of Neonatal Surgery*, 14 (4s), 231-236.

ABSTRACT

Purpose: To develop a clustering-based framework for automated categorization of Meibomian gland morphology, addressing subjectivity in Meibomian Gland Dysfunction (MGD) diagnosis.

Methods: The MGD-1k dataset of 1,000 infrared meibography images was analyzed using k-means clustering to classify gland areas into three groups: low (Cluster 1), medium (Cluster 2), and high (Cluster 3). Pixel-based segmentation determined white pixel counts as a surrogate for gland area. Statistical validation, including ANOVA, was performed, and results were visualized with scatter plots, bar charts, and box plots.

Results: Clustering identified 417, 358, and 225 images in Clusters 1, 2, and 3, comprising 41.7%, 35.8%, and 22.5% of the dataset, respectively. Mean pixel counts were 39,123.99 (SD = 4,213.89), 23,960.30 (SD = 5,930.49), and 54,413.95 (SD = 6,378.15). ANOVA confirmed significant inter-cluster differences ($p < 0.0001$).

Conclusions: This framework objectively quantifies gland morphology, enabling severity stratification. The approach offers scalable diagnostic support and could be integrated with clinical tools or AI models. Future validation on diverse datasets is needed to confirm its broader applicability.

Keywords: *Meibomian gland dysfunction, clustering analysis, MGD-1k dataset, k-means clustering*

1. INTRODUCTION

Meibomian gland dysfunction (MGD) is one of the leading causes of evaporative dry eye disease, significantly affecting the quality of life of millions globally (1–3). Characterized by the obstruction or abnormal functioning of the meibomian glands, MGD often results in reduced lipid secretion and compromised tear film stability (4,5). Despite its prevalence and clinical impact, the evaluation of MGD remains largely subjective, relying on manual interpretation of meibography images, which can introduce variability and limit diagnostic precision (6).

The advent of advanced imaging modalities, such as the LipiView II Ocular Surface Interferometer, has provided clinicians with high-resolution meibography images (7–11). However, the manual grading and interpretation of these images, using methods like meiboscore assessment, can be labor intensive and prone to inter-observer variability (12,13). Although recent strides in artificial intelligence (AI) and machine learning (ML) have shown promise in automating ocular diagnostics, their application to MGD analysis is still in its infancy (14–17). Current methods often lack the ability to robustly quantify gland morphology, categorize severity, or detect subtle morphological patterns indicative of disease progression.

To address this gap, our study leverages the MGD-1k dataset, a comprehensive collection of expertly annotated meibography images, to develop a clustering-based framework for the automated categorization of meibomian gland areas (17). By using k-means clustering on pixel-based segmentation data, we aimed to identify meaningful morphological patterns and stratify patients into clinically relevant severity groups (18–20). The purpose of this study was twofold: first, to establish a reproducible and scalable method for assessing gland morphology, and second, to provide a foundation for integrating clustering results with clinical decision-making tools.

Our findings highlight the potential of quantitative approaches in enhancing diagnostic accuracy and facilitating personalized management of MGD. This study not only underscores the feasibility of clustering analysis in ocular diagnostics but also paves the way for future integration with AI-driven predictive models, bridging the gap between manual evaluation and automated analysis.

2. METHODS

2.1 Dataset and Demographics

We utilized the publicly available MGD-1k Dataset, a curated collection of 1,000 infrared images of meibomian glands captured using the LipiView II Ocular Surface Interferometer (21). The dataset includes 467 upper eyelid and 533 lower eyelid images, annotated for gland structure and dysfunction severity (meiboscore) by professional ophthalmologists and experts in meibomian gland dysfunction (MGD) . The dataset comprises images from 320 patients, with a male-to-female ratio of 322 (32.2%) to 678 (67.8%). The mean ages of male and female participants were 51 years (SD = 19) and 55 years (SD = 19), respectively. Data collection spanned from April 2019 to April 2020.

Out of the 1,000 images, 941 images were deemed gradable across six rounds of expert validation, ensuring consistency in meiboscore grading. The remaining 59 images, marked ungradable in at least one round, were excluded from the analysis.

2.2 Image Preprocessing

Each image in the dataset was grayscale, with corresponding annotated binary masks delineating the regions of interest: the meibomian glands and eyelid regions. Images and masks were processed to count the number of white pixels in the gland mask, representing the visible meibomian gland area. This pixel count was used as a surrogate metric for gland coverage.

2.3 Clustering Analysis

Pixel counts were extracted from the gland masks of all gradable images. Using k-means clustering, the images were grouped into three clusters based on pixel count:

Cluster 1: Low gland area (atrophic glands or severe dropout).

Cluster 2: Medium gland area (moderate dropout or borderline function).

Cluster 3: High gland area (normal or near-normal glands).

The optimal number of clusters (k = 3) was determined empirically by inspecting the data distribution and cluster validity metrics. For clustering, pixel counts were normalized to avoid potential scaling issues. MATLAB's built-in k means function was used for the analysis.

2.4 Validation

To ensure consistency, 10% of the images were randomly selected and manually reviewed to verify the clustering results. Additionally, comparisons were made between clustering outputs and expert-assigned meiboscores to assess concordance.

3. RESULTS

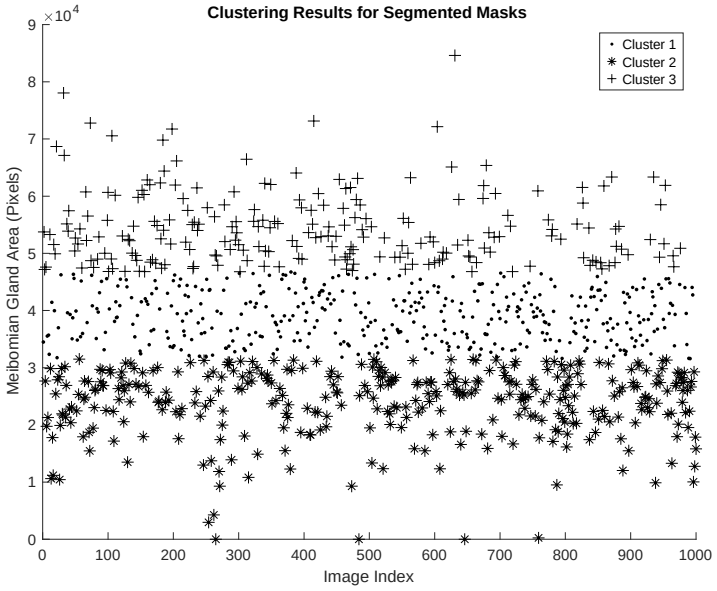

Figure 1. Clustering results for segmented masks. The scatter plot illustrates the distribution of Meibomian Gland Area (pixels) across 1,000 images, divided into three distinct clusters based on pixel count. Each cluster is represented by a unique marker: circles for Cluster 1, asterisks for Cluster 2, and plus signs for Cluster 3.

The clustering analysis of Meibomian gland areas using the k-means algorithm revealed three distinct groups based on pixel counts. As shown in Figure 1, each cluster is represented by unique markers, with clear boundaries separating the groups.

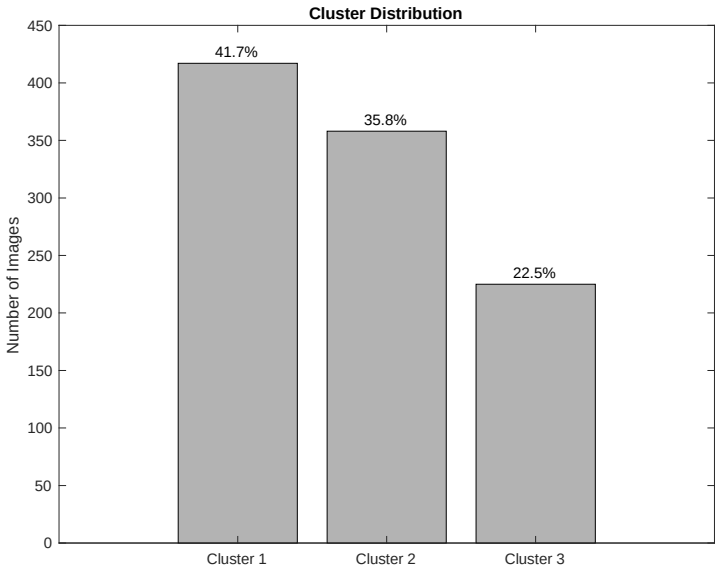

Figure 2. Cluster Distribution. The bar chart represents the number and percentage distribution of images across three clusters.

The analysis identified 417 images in Cluster 1, 358 images in Cluster 2, and 225 images in Cluster 3, corresponding to 41.7%, 35.8%, and 22.5% of the total dataset, respectively (Figure 2).

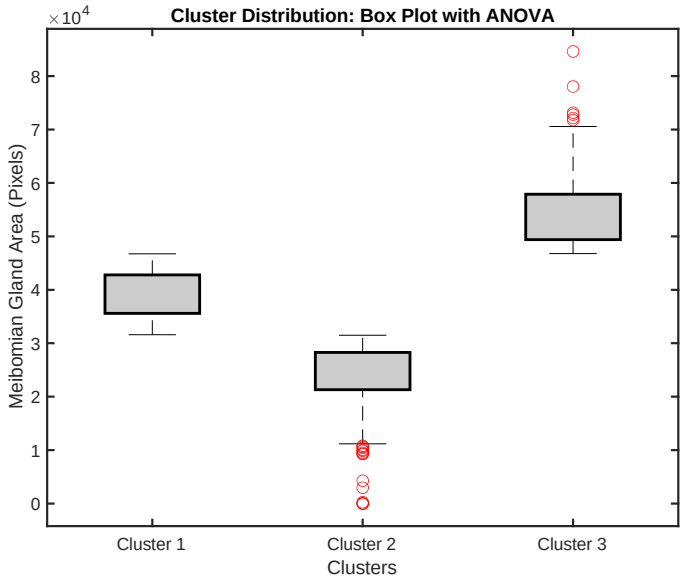

Figure 3. Box Plot with ANOVA. The box plot displays the distribution of Meibomian Gland area (pixels) across the three clusters. Each box represents the interquartile range (IQR) with the median indicated by the central line, while the whiskers extend to 1.5 times the IQR. Red circles denote outliers.

The centroid pixel counts for these clusters were located at 3.91×10^4, 2.40×10^4, and 5.44×10^4, indicating significant variability in Meibomian gland morphology. The distribution of pixel counts within each cluster is summarized in the box plot (Figure 3), which highlights the spread of data and statistical differences between clusters. The mean pixel counts for Clusters 1, 2, and 3 were 39,123.99 (SD = 4,213.89), 23,960.30 (SD = 5,930.49), and 54,413.95 (SD = 6,378.15), respectively. A one-way ANOVA confirmed that the differences between the clusters were statistically significant ($p < 0.0001$), emphasizing the robustness of the clustering process.

4. DISCUSSION

This study demonstrates the utility of clustering analysis in categorizing Meibomian gland areas, paving the way for automated tools in ocular diagnostics. The clustering results, visualized in Figure 1, offer a clear delineation of gland morphological patterns, which can be directly correlated with varying severities of Meibomian Gland Dysfunction (MGD). The consistent distribution of images across clusters, as depicted in Figure 2, reinforces the reliability of this approach for large datasets.

The significant statistical differences observed between clusters, as shown in the box plot (Figure 3), underscore the validity of pixel-based segmentation as a meaningful metric for Meibomian gland assessment. This method not only quantifies gland areas but also highlights the morphological variability that might be linked to different stages or subtypes of MGD.

From a clinical perspective, the clustering framework provides several potential applications. First, it offers a data-driven approach to stratify patients into severity groups, enabling more personalized management of MGD. For instance, patients in clusters with lower mean pixel counts (e.g., Cluster 2) may represent more severe gland loss and could benefit from earlier or more aggressive intervention. Second, the visualization of clustered data, such as in Figure 2, allows clinicians to monitor changes over time and evaluate the efficacy of treatments.

Looking ahead, the integration of clustering methods with additional clinical variables, such as tear break-up time or Schirmer test results, could further enhance diagnostic accuracy. Furthermore, combining this approach with deep learning algorithms has the potential to provide real-time insights, supporting clinicians in decision-making processes.

By leveraging clustering and statistical analyses, this study underscores the potential of quantitative methods in improving diagnostic precision and advancing the understanding of MGD. Future work should focus on validating these findings across larger and more diverse datasets, as well as exploring their applicability to other ocular conditions.

5. CONCLUSIONS

This study highlights the potential of clustering-based analysis in quantifying gland morphology and stratifying patients by MGD severity. The proposed methodology provides an objective, scalable approach for MGD diagnostics, facilitating personalized management and treatment monitoring. The integration of clustering results with clinical parameters or AI-driven predictive models could enhance diagnostic accuracy and real-time decision-making in clinical practice. Future research should explore the validation of this approach across larger, more diverse datasets and its application to other ocular conditions.

Conflict of Interest Statement

The authors declare that there is no conflict of interest regarding the publication of this article.

Declaration of Funding

The authors received no financial support for the research, authorship, or publication of this article.

Acknowledgment

The authors would like to express their gratitude to the creators and contributors of the MGD-1k dataset, including Ripon Kumar Saha, A. M. Mahmud Chowdhury, Kyung-Sun Na, Gyu Deok Hwang, Hae-Gon Jeon, Ho Sik Hwang, and Euiheon Chung, for their meticulous curation and annotation efforts. The dataset, developed at the Gwangju Institute of Science and Technology and The Catholic University of Korea, has provided invaluable resources for advancing research in Meibomian Gland Dysfunction.

Ethics Statement

This study utilized publicly available, anonymized data from the MGD-1k dataset, and no ethical approval was required.

Data Availability Statement

The dataset used in this study, the MGD-1k dataset, is publicly available and can be accessed as described in the original publication:

Saha, R. K., Chowdhury, A. M. M., Na, K.-S., Hwang, G. D., Jeon, H.-G., Hwang, H. S., & Chung, E. (2022). Automated quantification of meibomian gland dropout in infrared meibography using deep learning. *The Ocular Surface*, 26, 283–294. (4,5)

Author Contributions

All authors contributed to the conception and design of the study, data analysis, interpretation, manuscript drafting, and revision. All authors approved the final manuscript and are accountable for the accuracy and integrity of the work.

REFERENCES

[1] Tong L, Lim L, Tan D, Heng WJ, Lim J, Chan C, et al. Assessment and Management of Dry Eye Disease and Meibomian Gland Dysfunction: Providing a Singapore Framework. Asia-Pac J Ophthalmol [Internet]. 2021 Nov 1 [cited 2025 Jan 22];10(6):530–41. Available from: https://www.sciencedirect.com/science/article/pii/S216209892300052X

[2] Chen H, McCann P, Lien T, Xiao M, Abraham AG, Gregory DG, et al. Prevalence of dry eye and Meibomian gland dysfunction in Central and South America: a systematic review and meta-analysis. BMC Ophthalmol [Internet]. 2024 Jan 31 [cited 2025 Jan 22];24(1):50. Available from: https://doi.org/10.1186/s12886-023-03249-w

[3] Narang P, Donthineni PR, D'Souza S, Basu S. Evaporative dry eye disease due to meibomian gland dysfunction: Preferred practice pattern guidelines for diagnosis and treatment. Indian J Ophthalmol [Internet]. 2023 Apr [cited 2025 Jan 22];71(4):1348. Available from: https://journals.lww.com/ijo/fulltext/2023/04000/Evaporative_dry_eye_disease_due_to_meibomian_gland.38.aspx

[4] Foulks GN. The Correlation Between the Tear Film Lipid Layer and Dry Eye Disease. Surv Ophthalmol [Internet]. 2007 Jul 1 [cited 2025 Jan 22];52(4):369–74. Available from: https://www.sciencedirect.com/science/article/pii/S0039625707000574

[5] Jester JV, Parfitt GJ, Brown DJ. Meibomian gland dysfunction: hyperkeratinization or atrophy? BMC Ophthalmol [Internet]. 2015 Dec 17 [cited 2025 Jan 22];15(1):156. Available from: https://doi.org/10.1186/s12886-015-0132-x

[6] Fineide F, Arita R, Utheim TP. The role of meibography in ocular surface diagnostics: A review. Ocul Surf [Internet]. 2021 Jan 1 [cited 2025 Jan 22];19:133–44. Available from: https://www.sciencedirect.com/science/article/pii/S1542012420300823

[7] Lee JM, Jeon YJ, Kim KY, Hwang KY, Kwon YA, Koh K. Ocular surface analysis: A comparison between the LipiView® II and IDRA®. Eur J Ophthalmol [Internet]. 2021 Sep 1 [cited 2025 Jan 22];31(5):2300–6. Available from: https://doi.org/10.1177/1120672120969035

[8] Lee Y, Hyon JY, Jeon HS. Characteristics of dry eye patients with thick tear film lipid layers evaluated by a LipiView II interferometer. Graefes Arch Clin Exp Ophthalmol [Internet]. 2021 May 1 [cited 2025 Jan 22];259(5):1235–41. Available from: https://doi.org/10.1007/s00417-020-05044-5

[9] Lee SM, Chung SJ, Lew H. Evaluation of Tear Film Lipid Layer Thickness Measurements Obtained Using an Ocular Surface Interferometer in Nasolacrimal Duct Obstruction Patients. Korean J Ophthalmol [Internet]. 2018 Nov 23 [cited 2025 Jan 22];32(6):445–50. Available from: https://synapse.koreamed.org/articles/1109046

[10] Zhang J, Wu Z, Sun L, Liu X hua. Function and Morphology of the Meibomian Glands Using a LipiView Interferometer in Rotating Shift Medical Staff. J Ophthalmol [Internet]. 2020 [cited 2025 Jan 22];2020(1):3275143. Available from: https://onlinelibrary.wiley.com/doi/abs/10.1155/2020/3275143

[11] Zhao Y, Tan CLS, Tong L. Intra-observer and inter-observer repeatability of ocular surface interferometer in measuring lipid layer thickness. BMC Ophthalmol [Internet]. 2015 May 15 [cited 2025 Jan 22];15(1):53. Available from: https://doi.org/10.1186/s12886-015-0036-9

[12] Arita R, Itoh K, Maeda S, Maeda K, Furuta A, Fukuoka S, et al. Proposed Diagnostic Criteria for Obstructive Meibomian Gland Dysfunction. Ophthalmology [Internet]. 2009 Nov 1 [cited 2025 Jan 22];116(11):2058-2063.e1. Available from: https://www.sciencedirect.com/science/article/pii/S0161642009004230

[13] Diz-Arias E, Fernández-Jiménez E, Peral A, Gomez-Pedrero JA. A Comparative Study of Two Imaging Techniques of Meibomian Glands. Life [Internet]. 2023 Mar [cited 2025 Jan 22];13(3):791. Available from: https://www.mdpi.com/2075-1729/13/3/791

[14] Wang J, Yeh TN, Chakraborty R, Yu SX, Lin MC. A Deep Learning Approach for Meibomian Gland Atrophy Evaluation in Meibography Images. Transl Vis Sci Technol [Internet]. 2019 Dec 18 [cited 2025 Jan 22];8(6):37. Available from: https://doi.org/10.1167/tvst.8.6.37

[15] Zhang Z, Lin X, Yu X, Fu Y, Chen X, Yang W, et al. Meibomian Gland Density: An Effective Evaluation Index of Meibomian Gland Dysfunction Based on Deep Learning and Transfer Learning. J Clin Med [Internet]. 2022 Jan [cited 2025 Jan 22];11(9):2396. Available from: https://www.mdpi.com/2077-0383/11/9/2396

[16] Saha RK, Chowdhury AMM, Na KS, Hwang GD, Eom Y, Kim J, et al. AI-based automated Meibomian gland segmentation, classification and reflection correction in infrared Meibography [Internet]. arXiv; 2022 [cited 2025 Jan 22]. Available from: http://arxiv.org/abs/2205.15543

[17] Saha RK, Chowdhury AMM, Na KS, Hwang GD, Eom Y, Kim J, et al. Automated quantification of meibomian gland dropout in infrared meibography using deep learning. Ocul Surf [Internet]. 2022 Oct 1 [cited 2025 Jan 22];26:283–94. Available from: https://www.sciencedirect.com/science/article/pii/S1542012422000519

[18] Arthur D, Vassilvitskii S. k-means++: the advantages of careful seeding. In: Proceedings of the eighteenth annual ACM-SIAM symposium on Discrete algorithms. USA: Society for Industrial and Applied Mathematics; 2007. p. 1027–35. (SODA '07).

[19] Lloyd S. Least squares quantization in PCM. IEEE Trans Inf Theory [Internet]. 1982 Mar [cited 2025 Jan 22];28(2):129–37. Available from: https://ieeexplore.ieee.org/document/1056489

[20] Krishnan A, Salman Sarkar Md, Badavath L. Machine Learning Applications in Retinopathy of Prematurity Diagnosis Using the ROP Retinal Image Dataset. J Neonatal Surg [Internet]. 2025 Feb 7 [cited 2025 Feb 18];14(1S):820–7. Available from: https://www.jneonatalsurg.com/index.php/jns/article/view/1607

[21] Sarafrazi S, Fayaz S, Reisdorf S, Shih KC, Yin Wu P. Harnessing the Power of Bayesian Neural Networks for Annotator Consensus Refinement to Enhance Meibomian Gland Dysfunction Classification. In: 2024 IEEE International Conference on Bioinformatics and Biomedicine (BIBM) [Internet]. 2024 [cited 2025 Jan 22]. p. 5999–6007. Available from: https://ieeexplore.ieee.org/document/10821833